EXPLORATION OF MOLECULAR ORIENTATION IN 3D PRINTED PETG AND PCTG THROUGH POLARIZED RAMAN SPECTROSCOPY

Silas Martin* and Bryan C. Borders†

Department of Chemistry & Physics, University of South Carolina Aiken, Aiken, SC 29801

Abstract

Glycol-modified poly (ethylene terephthalate) (PETG) and poly (1,4-cyclohexylenedimethylene terephthalate-co-ethylene glycol) (PCTG) are two commonly used polymers in 3D printing that primarily differ in the amount of 1,4-cyclohexanedimethanol (CHDM) in the polymer chain. In this work, the Raman spectra of PCTG and PETG from multiple manufacturers are compared and polarized Raman spectra are used to determine the alignment of the polymers within the printed samples. It was found that the ratio of peaks at 853 cm^{-1} and 866 cm^{-1} correlates to the CHDM content of the polymer. The orientation of the polymers shows a slight dependence on the printing direction. The orientation changes upon annealing, becoming more aligned along the long axis of the samples. The degree to which the molecular orientation changes upon annealing is related to the CHDM content of the polymer.

†Corresponding author: bryan.borders@ usca.edu *Undergraduate researcher and co-author

Keywords: Raman spectroscopy, 3D printing, molecular orientation, PETG, PCTG

Received: July 31, 2026 Accepted: August 7, 22026 Revision received: August 10, 2026 Published: August19, 2026

Introduction

3D printing, a form of additive manufacturing, is a technique that fabricates physical objects from digital models by depositing successive layers of material to produce the final object. Extrusion-based 3D printing techniques, such as fused deposition modeling (FDM), are some of the most popular methods of 3D printing. Typically, in FDM 3D printing, a movable print head extrudes a molten or semi-molten material in predefined patterns onto a print bed. The print bed is moved incrementally in the vertical direction to allow the printing of subsequent layers. While in theory any thermoplastic can be 3D printed using this method, the physical characteristics of some materials make them better suited for FDM printing.

Poly(ethylene terephthalate) (PET) is one of the most widely utilized thermoplastics globally, owing to its excellent mechanical strength, chemical resistance, and thermal stability.[1–3] While PET can be used in 3D printing, it's high propensity for crystallization can result in warping, a loss of clarity, and increased brittleness.[4] Printing PET also requires relatively high temperatures between 255 and 275 °C. To overcome these limitations, a fraction of the ethylene glycol (EG) used in the synthesis of PET can be replaced with another diol, usually 1,4-cyclohexanedimethanol (CHDM). The polymers resulting from this modification are referred to as glycol-modified poly (ethylene terephthalate) or PETG, the structure of which can be seen in Figure 1. The bulky nature of the glycol modifier makes crystallization of PETG nearly impossible at processing temperatures.[5] Additionally, the modification tends to lower the printing temperature to between 230 and 255 °C. While the mechanical properties of PET and PETG are similar, PETG tends to be less brittle and will elongate to a greater extent before breaking.[1,6,7] It is worth noting that glycol modifiers other than CHDM can be used in the production of PETG.[8]

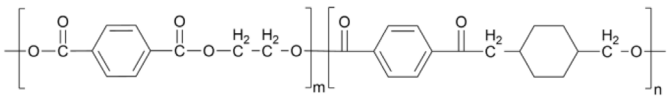

Figure 1. Molecular structure of PETG and PCTG. In PETG, m is greater than 50% whereas in PCTG m is less than 50%.

The exact properties of the modified polymer can be tuned by varying the mol% of the glycol modifier. A polymer will be classified as PETG when less than glycol modifier accounts for less than 50 mol% of the total diol content. For 3D printing applications, the CHDM content is typically between 30% and 45% of the total diol content.[1,9] When the CHDM content of the polymer is greater than 50% of the total diol content, the polymer then gets classified as poly (1,4-cyclohexylenedimethylene terephthalate-co-ethylene glycol) (PCTG). This high CHDM content offers even higher impact strength and ductility, making it increasingly popular in heavy-gauge sheet extrusion, medical devices, and rapid prototyping applications like fused deposition modeling (FDM) 3D printing.[3] The physical properties of these polymers depend not only the composition and level of crystallinity, but also the molecular orientation of the polymers.[8,10–12] Molecular orientation strongly impacts mechanical, optical, and electronic properties and therefore influences the potential applications of the polymer.

While the Raman signatures of PET and PETG have been extensively documented in literature, systematic comparative studies focusing on the Raman characterization of PCTG remain sparse. Understanding how the higher concentration of CHDM influences the Raman spectra, specifically the polarization dependence of specific vibrational tensors, is essential for accurately modeling strain-induced orientation and structural evolution during manufacturing.

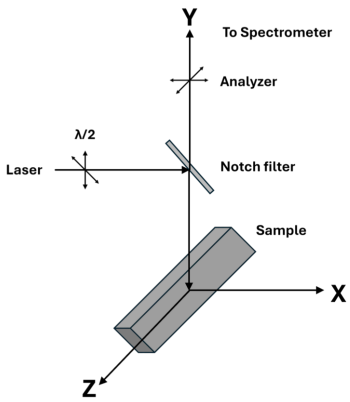

Figure 2. Coordinate system used to record polarized Raman spectra

In this work, comparative analysis of the polarized and non-polarized Raman spectra of PETG and PCTG was performed. Due to variability in composition, samples of PETG from multiple manufacturers were included in this study. In addition to comparing the characteristic peaks of the Raman spectra, the orientation parameter $\langle P_2 \rangle$ was determined using the most probable distribution (MPD) method described by Richard-Lecroix et al.[13] The value of $\langle P_2 \rangle$ correlates with the alignment of a given Raman tensor with the direction of the long axis of the sample, Z in Figure 2. A $\langle P_2 \rangle$ value of 0 corresponds to a completely isotropic distribution, a value of 1 corresponds to perfect alignment along the Z-axis, and a value of -0.5 corresponds to perfect alignment perpendicular to the long axis (the X-axis). This analysis was performed before and after annealing as well as along both the horizontal (Z) and vertical (X) print directions. These insights provide a framework for non-destructive in-situ monitoring of molecular alignment and structural anisotropy in terephthalate-based co-polyester systems.

Experimental Methods

Sample preparation:

All test pieces were printed on either a Bambu Lab P1S or an A1 Mini. Both Printers were equipped with a 0.4 mm, hardened steel nozzle and all models were sliced and prepared for printing using Bambu Studio. Samples were printed with a 0.2 mm layer height, three bottom layers, five top layers, and two perimeters with a 15% infill. The maximum volumetric speed was limited to 12 $mm^3 \cdot s^{-1}$. The bed temperature was set to 70 °C while the nozzle temperature was set to 255 °C.

Dimensions for the test sample were 25 x 5 x 5 mm^3 and top surface of the samples were printed in a concentric pattern with the infill following the same pattern. A rectangular pattern was chosen to easily distinguish between regions print directions. Samples were printed from filaments obtained from Matter Hackers, Overture 3D, HatchBox, and Polymaker. The specific filaments and batch numbers are listed in Table 1. All filaments were purchased directly from the manufacturers, had a diameter of 1.75 mm, and were used without any modification. A PET standard was used as a reference point to help identify peaks coming from the glycol modifiers and other additives in the 3D printing filaments.

Instrumentation:

All Raman spectra were collected using a XploRA PLUS (Horiba, Kyoto, Japan) micro-spectrometer with a 785 nm excitation laser and a 50x objective. The spectrometer was equipped with 600 g/mm, 1200 g/mm and 1800 g/mm gratings. The 600 g/mm grating was used to collect polarized spectra while the 1800 g/mm grating was used to collect high resolution spectra. Laser power at the sample was 35 mW. The spectrometer was equipped with a half-waveplate to control polarization of the incident light as well as a polarization analyzer in front of the detector. Figure 2 shows the coordinate system used to define the polarizations in these experiments. Briefly, the Z-direction is defined as the long axis of the sample, X is the short axis, and Y is the direction of incident light. This coordinate system was chosen to be consistent with the analysis used by Richard-Lacroix et al.[13] Spectra were collected in the following polarizations given in Porto notation: Y(ZZ)Y, Y(ZX)Y, Y(XZ)Y, and Y(XX)Y. Spectra were collected both in regions on the sample where the printhead was moving in the Z-direction and in regions where the printhead was moving in the X-direction to determine the dependence of molecular orientation on print direction. Raman spectra were also collected before and after annealing. Samples were annealed by slowly heating to a temperature of 110 °C, holding the temperature for four hours, then allowing the samples to slowly cool to room temperature overnight. The annealing temperature was chosen because the glass transition temperature of PETG is approximately 80º C.

Table 1. Materials used in this work, including batch number where available

Manufacturer	Material	Batch Number
Matter Hackers (MH)	PETG Pro	041200
	PCTG	131-051425-09AW
Hatchbox (HB)	PETG	N/A
Overture	PETG	VC04BC0802
Polymaker (PM)	Polylite PETG	A260420283

Correction factors were applied to all spectra to compensate for the residual polarization dependence of the spectrometer. Correction factors were determined by recording polarized spectra of carbon tetrachloride which has peaks with established depolarization ratios.[14]

Data analysis:

$\langle P_2 \rangle$ values were calculated based on the 1615 cm^{-1} peak. This peak was chosen for several reasons. First, the peak arises from C=C stretches in the benzene ring of the terephthalate and is therefore present in all samples. Second, the Raman tensor of this vibrational mode is aligned along the C_1-C_4 axis of the benzene ring with a tilt angle of 20° with respect to the polymer chain.[13,15] Because the methods of measuring $\langle P_2 \rangle$ using Raman spectroscopy truly measure the orientation of the Raman tensors relative to the long axis of the sample, it is important to pick a vibrational mode with a tensor closely aligned to the molecular axis. Finally, the peak at 1615 cm^{-1} is strong and gives sufficient signal-to-noise ratios without having to rely on long integration times.

$\langle P_2 \rangle$ values were calculated by first calculating the depolarization ratios using the equations

$$\rho_1 = \frac{I_{ZX}}{I_{ZZ}} \qquad (1a)$$

and

$$\rho_2 = \frac{I_{XZ}}{I_{XX}} \qquad (1b)$$

where I_{ij} describes the intensity of the 1615 cm^{-1} band under the ij polarization. The depolarization ratios were then used to solve a series of equations described elsewhere.[13,16] These equations were solved using Mathcad.

Results and Discussion

Comparison of non-polarized Raman spectra:

Figure 3a shows the Raman spectra of the 3D printed samples. Peak assignments are shown in Table 2. The most significant differences can be seen in the 750-950 cm^{-1} region (Figure 3b). The peak at 856 cm^{-1} corresponds to the C-O stretching mode (present in all samples) while the peak at 866 cm^{-1} corresponds to a ring breathing C-C stretching mode from the cyclohexyl group.[8,17,18] While the referenced sources do not distinguish between these

two peaks, the peak at 856 cm^{-1} is easily identifiable by looking at the PET spectrum which has no CHDM present. The intensity at 866 cm^{-1} is strongest in PCTG which has the highest CHDM content, further supporting this assignment. This region contains other notable differences as well. The O-C(O)-O stretching mode at 772 cm^{-1} is present all samples except the PET standard and the Overture PETG sample. The CH_2 rocking peak at 884 cm^{-1}, which comes from the EG units, is strongest in PET and weakest in PCTG. The intensity of this peak is consistent with the different EG content in the polymers studied.

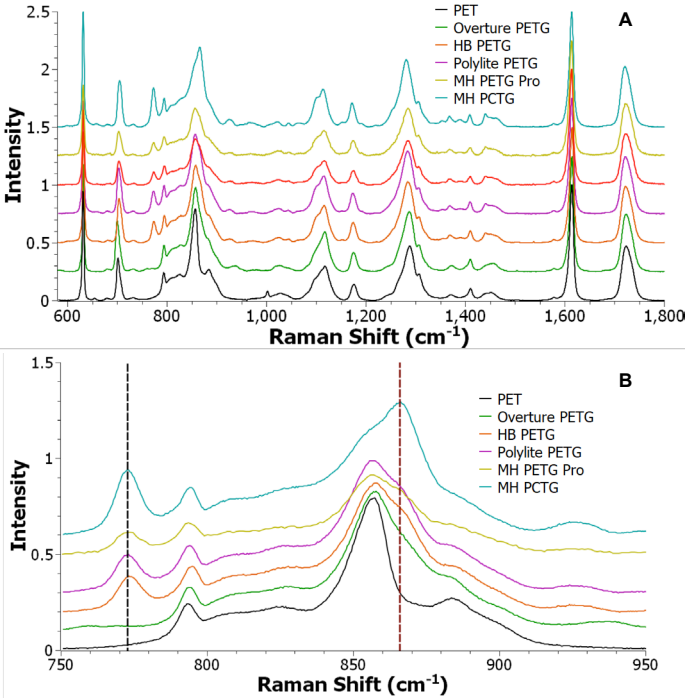

Figure 3 a) Raman spectra of the different materials used in this study. b) Close up of the 750 – 950 cm^{-1} region of the spectrum highlighting the differences between the materials. Spectra have been offset for clarity. Dotted lines added for emphasis.

Table 2. Assignment of significant Raman peaks. Abbreviations: m, moderate; s, strong; sh, shoulder; w, weak; v, very

Raman Shift (cm^{-1})	Assignment
3082 w	CH stretching
3068 w	CH stretching
3000 w	CH stretching
2960 w	CH_2 stretching
1730 m	C=O stretching
1615 s	C=C stretching (ring)
1450 w	CH deformation
1412 vw	C-C stretching (ring)
1370 vw	CH_2 wagging
1282 m	C-C stretching (ring), C-O stretching
1270 m	C-C stretching (ring), C-O stretching
1245 sh, w	C-C stretching (ring), C-O stretching
1175 w	CH in-plane bending (ring)
1038 vw	C-C stretching (glycol)
890 vw	CH_2 rocking
866 m	C-C stretching (ring breathing, CHDM)
856 m	C-O stretching
797 w	CH out-of-plane bending (ring)
772 m	O-C(O)-O stretching
703 m	C-H out-of-plane bending
631 s	Phenyl ring vibration

The above data suggest that it should be possible to determine the EG/CHDM ratios using Raman spectroscopy. The largest hurdle to this analysis is the proprietary nature of the polymer blends used in the filaments. While it is possible to determine these ratios via NMR, the ease of sample preparation and ability to reanalyze samples makes Raman analysis a more attractive option to optimize.[9]

The differences between the PETG sample from Overture and the other PETG samples suggest that glycol modifier used in the Overture filament was not CHDM. While Yost et al. determined the Overture PETG had a CHDM content of 21.0%, Overture 3D changed their PETG formulation at the end of 2025.[9,19] It was confirmed with Overture 3D that the batch number of the filament used in this study corresponds to batches produced after the formulation change.

While further experimentation is necessary to quantify the CHDM content using Raman spectroscopy, qualitative data can still be obtained looking at the peaks around 860 cm^{-1}. Table 3 shows the ratios of the intensities at 866 cm^{-1} to 856 cm^{-1}. The MH PCTG had the highest ratio, which is consistent with it having the highest CHDM content while the HB PETG has the smallest ratio, suggesting it has the lowest CHDM content. This is consistent with the study by Yost which showed HB PETG had the lowest CHDM content of the brands studied.[9] The PETG from Overture was omitted from this analysis as the Raman spectra suggest it does not contain CHDM.

The peak around 700 cm^{-1} (Figure 4), which corresponds to a C-H out-of-plane bending mode, also appears to show a CHDM dependence. In PET this peak is located at 701 cm^{-1} whereas in PCTG it is located at 705 cm^{-1}. The peaks for the MH, HB, and PM samples are located in between at 703 cm^{-1}. Interestingly, the peak for the Overture sample is shifted to 699 cm^{-1}. While this band clearly has a dependence on the CHDM content of the polymer, the changes are small enough that use of a very high-resolution spectrometer would be necessary to quantify the relationship.

Table 3. Ratios of the intensities at 866 cm^{-1} peak to the 856 cm^{-1} peak.

Material	I_{866}/I_{853}
MH PETG Pro	0.28
PM Polylite PETG	0.29
HB PETG	0.21
MH PCTG	1.8

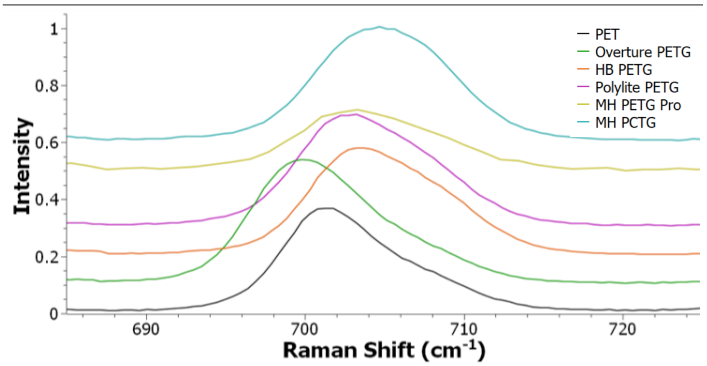

Figure 4 Close up of the 700 cm^{-1} region of the Raman spectrum. Spectra have been offset for clarity

$\langle P_2 \rangle$ determination and molecular orientation analysis:

Table 4 shows the results of the $\langle P_2 \rangle$ calculations for unannealed samples taken in both the X- and Z- printing directions. In the Z-direction, all samples had $\langle P_2 \rangle$ values between -0.1 and -0.2, corresponding to molecular alignment between isotropic and oriented in the X-direction. Similar values were obtained looking at regions of the samples in the X-printing direction. Table 4 also shows the difference between the $\langle P_2 \rangle$ values measured in the X-direction and the values measured in the Z-direction. $\Delta\langle P_2 \rangle$ was calculated as

$$\Delta\langle P_2 \rangle = \langle P_2 \rangle(X) - \langle P_2 \rangle(Z) \qquad (2)$$

The $\Delta\langle P_2 \rangle$ values show that for most samples, alignment of the polymers has a slight dependence on the printing direction, with most samples showing a more isotropic alignment while printed in the X-direction. The MH PETG Pro showed the largest difference between alignment in print directions.

Because polymers are poor conductors of heat, 3D printed samples are cooled unevenly during extrusion, leading to internal stresses. The goal of annealing polymers is to relieve these stresses by heating the polymers to above their glass transition temperatures. Doing so allows the molecular chains to rearrange, thereby relieving the internal stresses.[20,21] Table 5 shows the calculated $\Delta\langle P_2 \rangle$ values of samples before and after annealing. For consistency, all calculations were performed using measurements taken along the Z-printing direction. Again a difference in $\langle P_2 \rangle$ was calculated using the equation

$$\Delta\langle P_2 \rangle = \langle P_2 \rangle(Annealed) - \langle P_2 \rangle(Unannealed) \qquad (3)$$

Table 4. Comparison of $\langle P_2 \rangle$ values obtained by looking at the 1615 cm^{-1} peak. Values were calculated for measurements made in both the X and Z printing directions.

Material	Z-Direction Unannealed	X-Direction Unannealed	$\Delta\langle P_2 \rangle$
MH PETG Pro	-0.180	-0.048	0.132
PM Polylite PETG	-0.113	-0.055	0.058
HB PETG	-0.166	-0.111	0.055
Overture PETG	-0.119	-0.122	-0.003
MH PCTG	-0.139	-0.103	0.036

Table 5. Comparison of $\langle P_2 \rangle$ values calculated from the 1615 cm^{-1} peak before and after annealing. All data were collected from the Z print direction

Material	Unannealed	Annealed	$\Delta\langle P_2 \rangle$
MH PETG Pro	-0.180	0.011	0.191
PM Polylite PETG	-0.113	0.145	0.258
HB PETG	-0.196	0.102	0.298
Overture PETG	-0.119	-0.024	0.095
MH PCTG	-0.139	-0.176	-0.037

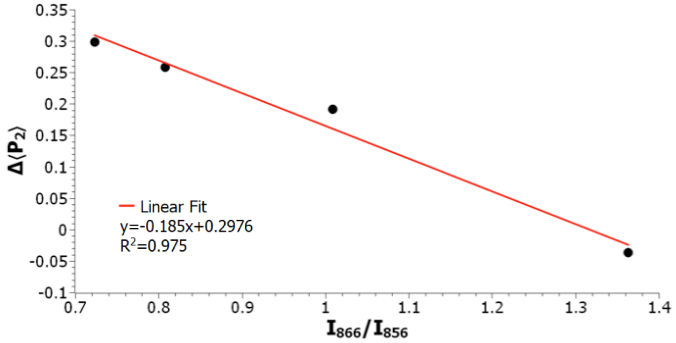

Figure 5 Plot of Δ $\langle P_2 \rangle$ vs the ratio of the 866 cm^{-1} to 856 cm^{-1} peaks as a result of annealing

For most samples, the $\langle P_2 \rangle$ value increased after annealing, corresponding to greater alignment along the Z-direction. The HB PETG sample showed the greatest change while the MH PETG Pro sample showed the smallest change. The MH PCTG showed a decrease in $\langle P_2 \rangle$ upon annealing. There is a correlation between the I_{866}/I_{856} ratio and $\Delta\langle P_2 \rangle$ shown in Figure 5. This shows that there is a relationship between CHDM content and how molecular alignment changes upon annealing. The above analysis was also performed on data collected along the X-direction of the samples and similar results were observed.

Even though PETG is an amorphous material that is nearly impossible to crystallize, annealing still affects the properties of the polymer. Hart et al found that annealing amorphous thermoplastics dramatically increased their fracture toughness.[22] This change is likely due to the release of residual thermal stresses that occur during the manufacturing process. The above analysis of the $\langle P_2 \rangle$ values can help elucidate how stresses, thermal and otherwise, are related to the molecular ordering of the polymer.

Conclusion

In this work, the Raman spectra of PETG from several manufacturers and PCTG were compared. It was found that ratio of the peaks at 866 cm^{-1} and 856 cm^{-1} correlate to the CHDM/EG ratio in the polymer, but more work is needed to develop a quantitative relationship. The MPD method of determining the orientation factor $\langle P_2 \rangle$ was used to determine the orientation of the polymers within the samples. It was shown that the orientation of most of the polymers shows some dependence on printing direction. Annealing changes the molecular orientation of the polymers, and the degree to which the change occurs shows a strong dependence on the CHDM content of the polymer. This work represents a step toward an increased understanding of how molecular orientation is related to internal stresses in 3D printed materials.

Acknowledgement

Funding for this project was provided by the U.S. Department of Energy through the Workforce Opportunities in Regional Careers (WORC) initiative of the Savannah River Site Community Reuse Organization.

References

1. Dupaix, R. B.; Boyce, M. C. *Polymer* **2005**, *46* (13), 4827–4838.
2. Holcomb, G.; Caldona, E. B.; Cheng, X.; Advincula, R. C. *MRS Commun.* **2022**, *12* (3), 381–387.
3. Wang, H.; Zheng, H.; Jiang, J.; Zhao, L.; Xi, Z. *Ind. Eng. Chem. Res.* **2024**, *63* (13), 5729–5741.
4. Toth, L.; Slezák, E.; Bocz, K.; Ronkay, F. *Mater. Today Sustain.* **2024**, *26*, 100757.
5. Spina, R. *Sci. Rep.* **2026**, *16* (1), 18592.
6. Ramírez-Revilla, S.; Camacho-Valencia, D.; Gonzales-Condori, E. G.; Márquez, G. *MRS Commun.* **2023**, *13* (1), 55–62.
7. Zisopol, D. G.; Minescu, M.; Iacob, D. V. *Eng. Technol. Appl. Sci. Res.* **2024**, *14* (2), 13487–13492.
8. Kozlova, L. Yu.; Mendeleev, D. I.; Vasimov, D. D.; Kozlov, V. A.; Nikolaeva, G. Yu.; Moskovskiy, M. N.; Gudkov, S. V.;

Novikov, V. S. *J. Raman Spectrosc.* **2026**, *57* (3), 544–555.
9. Yost, S. F.; Smith, J. C.; Vogt, B. D. *Macromol. Mater. Eng.* **2026**, *311* (1), e00307.
10. Bouita, M.; Tinnes, J.-P.; Bourson, P.; Malfois, M.; Ponçot, M. *J. Raman Spectrosc.* **2023**, *54* (2), 225–232.
11. Yang, S.; Michielsen, S. *Macromolecules* **2002**, *35* (27), 10108–10113.
12. Ward, I. M. *Structure and Properties of Oriented Polymers*; Springer Science & Business Media, 2012.
13. Richard-Lacroix, M.; Pellerin, C. *Macromolecules* **2013**, *46* (14), 5561–5569.
14. Ikawa, S.; Whalley, E. *J. Chem. Phys.* **1988**, *89* (1), 51–54.
15. Lesko, C. C. C.; Rabolt, J. F.; Ikeda, R. M.; Chase, B.; Kennedy, A. *J. Mol. Struct.* **2000**, *521* (1), 127–136.
16. Richard-Lacroix, M.; Pellerin, C. *App. Spec.* **2013**, 67 (4), 409-419
17. Nicita, F.; D'Amico, C.; Filardi, V.; Spadaro, D.; Aquilio, E.; Mancini, M.; Fiorillo, L. *Eur. J. Dent.* **2023**, *18* (1), 228–235.
18. Petousis, M.; Michailidis, N.; Saltas, V.; Papadakis, V.; Spiridaki, M.; Mountakis, N.; Argyros, A.; Valsamos, J.; Nasikas, N. K.; Vidakis, N. *Nanomaterials* **2024**, *14* (9), 761.
19. *Introducing Overture3D New PETG Filament: Prints the Way It Should*. Overture 3D. https://overture3d.com/blogs/overture-blogs/introducing-overture3d-new-petg-filament (accessed 2026-07-27).
20. Yalkin, H.E.; Ozkan, A.N. *Polymer Engineering & Science.* **2026**, 66, 4995-5006
21. Butt, J.; Bhaskar, R. *J. Manuf. Mater. Process.* **2020,** 4(2), 38
22. Hart, K. R.; Dunn, R. M.; Sietins, J. M.; Hofmeister Mock, C. M.; Mackay, M. E.; Wetzel, E. D. *Polymer* **2018**, *144*, 192–204.